ORNL/TM-2011/516

DFT STUDY REVISES INTERSTITIAL CONFIGURATIONS IN HCP Zr

November 2011

G.D. SAMOLYUK
Oak Ridge National Laboratory

S. I. GOLUBOV
Oak Ridge National Laboratory

Y.N. OSETSKY
Oak Ridge National Laboratory

R. E. STOLLER
Oak Ridge National Laboratory

DOCUMENT AVAILABILTY

Reports produced after January 1, 1996, are generally available free via the U.S. Department of Energy (DOE) Information Bridge.

Web site http://www.osti.gov/bridge

Reports produced before January 1, 1996, may be purchased by members of the public from the following source.

National Technical Information Service
5285 Port Royal Road
Springfield, VA 22161
Telephone 703-605-6000 (1-800-553-6847)
TDD 703-487-4639
Fax 703-605-6900
E-mail info@ntis.gov
Web site http://www.ntis.gov/support/ordernowabout.htm

Reports are available to DOE employees, DOE contractors, Energy Technology Data Exchange (ETDE) representatives, and International Nuclear Information System (INIS) representatives from the following source.

Office of Scientific and Technical Information
P.O. Box 62
Oak Ridge, TN 37831
Telephone 865-576-8401
Fax 865-576-5728
E-mail reports@osti.gov
Web site http://www.osti.gov/contact.html

ORNL/TM-2011/516

Materials Science and Technology Division

DFT STUDY REVISES INTERSTITIAL CONFIGURATIONS IN HCP Zr

G.D. SAMOLYUK
Oak Ridge National Laboratory

S. I. GOLUBOV
Oak Ridge National Laboratory

Y.N. OSETSKY
Oak Ridge National Laboratory

R.E. STOLLER
Oak Ridge National Laboratory

December 2011

Prepared by
OAK RIDGE NATIONAL LABORATORY
Oak Ridge, Tennessee 37831-6283
managed by
UT-BATTELLE, LLC
for the
U.S. DEPARTMENT OF ENERGY
under Contract DE-AC05-00OR22725

CONTENTS

LIST OF FIGURES

Figure

LIST OF TABLES

Tables

ACKNOWLEDGEMENTS

We are grateful to Dr. A. Barashev for useful discussion. This research used resources of the National Energy Research Scientific Computing Center, which is supported by the Office of Science of the U. S. Department of Energy. Work was supported by the Consortium for Advanced Simulation of Light Water Reactors (http://www.casl.gov), an Energy Innovation Hub (http://www.energy.gov/hubs) for Modeling and Simulation of Nuclear Reactors under U.S. Department of Energy Contract No. DE-AC05-00OR22725

ABSTRACT

Analysis of experimental results on microstructure evolution in irradiated Zr and Zr alloys has demonstrated that existing information on self-interstitial defects in Zr is in contradiction with material behavior. We initiated an extensive theoretical and modelling program to clarify this issue. In this report we present *ab initio* calculations of single self-interstitial atoms (SIA) in Zr. We demonstrate the importance of simulation cell size, type of exchange-correlation functional and *c/a* ratio used. The results obtained demonstrate that the most stable SIA configurations lie in the basal plane and provide evidence for enhanced interstitial transport along basal planes. The results will be used to develop a new interatomic potential for Zr to use in large-scale atomistic modelling of mechanisms relevant for radiation-induced microstructure evolution.

1. INTRODUCTION

Zirconium alloys are widely used in the nuclear industry because of their low absorption cross-section for neutrons. Irradiation-induced growth and creep, i.e. change in shape at constant volume, are the important modes of dimensional instability in these materials and a major concern in thermal nuclear PWR or BWR reactors. It is commonly accepted that the instability takes place via condensation of self-interstitial atoms (SIAs) into dislocation loops lying on the prism planes, while vacancies form loops on the basal planes, which is equivalent to transfer of atoms from the basal to the prism planes. Thus, properties of the mobile defects, their configurations and diffusion modes, are important for predictive models of the phenomena of interest. The properties of vacancies are relatively simple and have been studied extensively, whereas the situation with the SIAs is more complicated. Indeed, the latter may exist in different configurations and, what is even more important, have different diffusion modes, e.g. they migrate three-dimensionally (3-D) if the dumbbell configuration is the most stable, or one-dimensionally (1-D) in the case when they are in the crowdion configuration as has been shown for cubic crystals. Figure 1 illustrates the seven possible configurations for a SIA defect in hexagonal closed packed (hcp) structure as discussed in the Table 1.

Since the reaction kinetics of 3-D and 1-D diffusing defects are different, of the second order in the case 3-D and third for 1-D diffusion, it is important to know the SIA configuration in Zr [1]. The so-called *ab initio* methods provide the most accurate way to calculate the properties of simple defects in metals. So, calculations of point defects in Zr have been performed by Willaime [2] and Domain *et al*. [3] and both resulted in a conclusion that the octahedral is the most stable configuration for the SIA, and this SIA will execute 3-D diffusion. However, this result contradicts some observations irradiated pure Zr [4]. It was found that during irradiation with 1 MeV electrons, vacancy loops and voids were mostly aligned in rows parallel with the basal planes at low and high temperature, respectively. This is similar to void lattice formation in bcc and fcc metals, which is commonly attributed to the presence of 1-D SIA diffusion (see e.g. [5, 6]). Since the primary damage produced in Zr irradiated with 1 MeV electrons consists of single vacancies and SIAs only, it is reasonable to assume that the alignment of vacancy type defects originate from the diffusion of SIAs parallel to the basal planes. Such diffusion cannot be attributed to the octahedral SIA configuration (see Fig. 1 for reference to configurations). Therefore, one may doubt the validity of calculations in [2, 3]. There may be two reasons for the inaccuracy: (a) the size of simulation boxes might be too small and/or (b) a deviation of the *c/a* ratio obtained in the calculations (1.600 in [2] and 1.603 in [3]) from the experimental value: 1.593. Indeed, the maximum size of the box in the crowdion direction used in [1, 2] was only four lattice parameters, whereas similar calculations in bcc and fcc metals (see e.g. [7-9]) demonstrated that the effective crowdion size is more than ten lattice parameters. If the effective

size of the crowdion in Zr on the same scale, one may expect that their formation energy in the small size box could be overestimated in [2, 3] and, consequently, their relative stability underestimated. One may also expect that correction of the *c/a* ratio to a lower value would have a similar effect and lead to stabilization of SIA configuration in the basal planes. The relative stability of SIAs in different configurations is also used for designing interatomic potentials (see e.g. [10]) for MD simulations, it is clear that *ab initio* calculations have to account for the limitations discussed to clarify these issues.

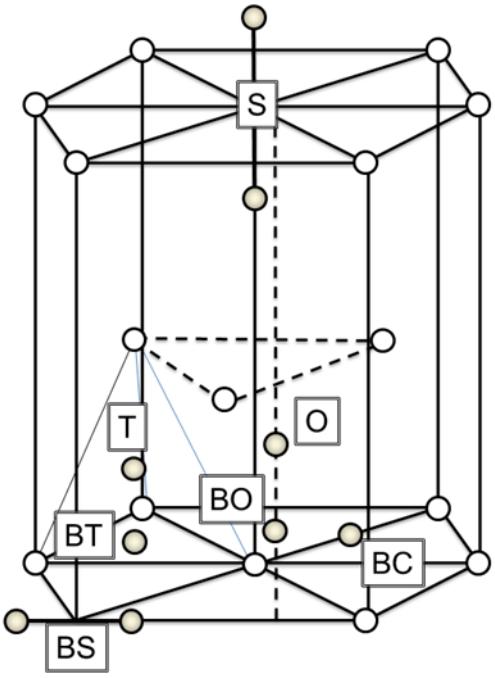

Figure 1 The most typical configurations of self-interstitial atom in the HCP lattice.

Table 1 SIA configurations in hcp lattice.

BO	Basal octahedral	Octahedral configuration in basal plane
BS	Basal split	Dumb-bell configuration along *a* direction in basal plane
BC	Basal crowdion	Crowdion configuration along *a* direction in basal plane
BT	Basal tetrahedral	Tetrahedral configuration in basal plane
O	Octahedral	Octahedral configuration out of basal plane
S	*c*-split	Dumb-bell configuration along *c* direction
T	Tetrahedral	Tetrahedral configuration out of basal plane

The results obtained in [2, 3] for supercells of 3×3×2 and 4×4×3 unit cells, containing 37 and 97 atoms, respectively are presented in Table 2. As can be seen, there is a noticeable difference between local density (LDA) and generalized gradient approximations (GGA) exchange-correlation (XC) functional results. The most stable configuration corresponds to the basal octahedron (BO) [2]. However, the GGA results for both supercell sizes predict the octahedral SIA is the most stable. Also, the LDA value for the formation energy of the S-type configuration is very close to the octahedron (O) and BO configurations. This reduction of non-basal split (S) defect formation energy can be seen [2] with increasing equilibrium *c*/*a* parameter up to 1.615 in the LDA calculation (Table 3). The GGA result for *c*/*a* varies between 1.6 [2] and 1.603 [3]. Since the defect formation energy is very sensitive to the *c/a* ratio, below we the consider results obtained using GGA only.

Although the increase of supercell size from 37 to 97 atoms does not change the type of most stable SIA configuration ([3] and Table 2), it's still in octahedral position, the formation energies of basal configurations BO and basal split (BS) decrease much faster compared to the non-basal one. This is a clear indication that the calculations presented in [2, 3] did not converge and further increase of the cell should change the relative stability of configurations.

Table 2. The published results for the defect formation energy (in eV) obtained for supercells of two sizes with corresponding number of atoms (N) and XC functional. The energies of formation of all types of defects are presented relative to O-type SIA formation energy and O-configuration is in eV.

XC	Ref.	supercell size (N)	E_O	E_S-E_O	E_C-E_O	E_{BO}-E_O	E_{BS}-E_O
LDA	[2]	3×3×2 (37)	2.73	0.22	0.45	0.24	0.50
GGA	[2]	3×3×2 (37)	3.04	0.24	0.48	0.10	0.35
GGA	[3]	3×3×2 (37)	2.83	0.30	0.36	0.24	0.40
LDA	[2]	4×4×3 (97)	2.79	0.01	0.28	-.01	0.11
GGA	[3]	4×4×3 (97)	2.84	0.17	0.24	0.04	0.11

2. RESULTS AND DISCUSSION

In our study we performed electronic structure calculations using the quantum-espresso (QE) [11] and Vienna *Ab initio* Simulation Package (VASP) [12] packages within framework of DFT using the GGA approximation for the exchange-correlation energy. The calculations have been performed using plane-wave basis set and ultrasoft pseudopotential [13]. Complete description of the pseudopotentials used can be found in [1, 2]. We used Perdew, Burke and Ernzerhof (PBE) [14] XC functional in QE calculation and Perdew, Wang (PW) [15] in VASP. The plane wave energy cutoffs of 26 Ry and 16.5 Ry were used in QE and VASP calculation, respectively. The Brillouin zone (BZ) summation was carried out over 6×6×6, 4×4×4, 3×4×4 or 2×4×4 BZ grids for 3×3×2, 4×4×3, 6×4×3, 8×4×3 and 10×4×3 supercells, respectively, and the structure was relaxed until the convergence in energy of 0.0015 Ry was reached. Following previous calculations [2], we modify size and shape of the supercell with a defect using isotropic scaling by a factor $\left[(N+1)/N\right]^{1/3}$, where N is the number of atoms in a perfect supercell. Such a procedure allows the pressure to be kept close to zero with the accuracy better than 1 kBar. We considered only the most stable configurations which are important for diffusion of the SIA: O, BO and BS. The details of our present and previous [2, 3] calculations together with the corresponding equilibrium *c/a* ratios are summarized in Table 3.

Table 3. The details of calculation together with corresponding equilibrium lattice parameters. BZ grid is presented for supercell 3×3×2.

Ref.	XC	e_{cut} (Ry)	BZ grid	*a* (Å)	*c*/*a*
[2]	GGA PW [15]	16.5	4×4×6	3.23	1.603
[1]	LDA PZ [16]	20.0	6×6×6	3.15	1.615
[1]	GGA PBE [14]	20.0	6×6×6	3.23	1.600
Present QE	GGA PBE [14]	26.0	6×6×6	3.23	1.600
Present VASP	GGA PW [15]	16.5	6×6×6	3.23	1.603

The results for a small cell of 37 atoms are close to those in [2] and [3] with the GGA (compare results in Tables 2 and 4) and demonstrate the same order in stability of different SIA

configurations. The small difference observed can be attributed to small differences in the calculations.

Table 4. The results for the defects formation energy (in eV) obtained for supercells of two sizes with the corresponding number of atoms (N) and XC functional. The formation energies of all types of defects are presented relative to O-type defect formation energy and the O configuration is in eV.

XC	Used package	scell (N)	E_O	E_S-E_O	E_{BO}-E_O	E_{BS}-E_O
GGA	QE	3×3×2 (37)	3.00	0.32	0.14	0.43
GGA	VASP	3×3×2 (37)	2.94	0.37	0.23	0.55
GGA	QE	4×4×3 (97)	2.97	0.13	-0.07	0.06
GGA	QE	6×4×3 (145)	2.92	0.10	-0.15	-0.02
GGA	VASP with exp. *c*/*a*	6×4×3 (145)	2.77	0.24	-0.07	0.04
GGA	VASP	6×4×x3 (145)	2.80	0.18	-0.07	0.05
GGA	QE	8×4×3 (193)	2.93	0.10	-0.17	-0.05
GGA	QE	10×4×3 (241)	2.93	0.09	-0.18	-0.06
GGA	QE with exp. *c*/*a*	10×4×3 (241)	2.93	0.12	-0.19	-0.09
GGA	QE	6×5×5(301)	2.91	0.06	-0.16	-0.02

For the 4×4×3 cell, the calculated ground state changed from O to BO configuration while the relative formation energy for BS (E_{BS}-E_O) reduced by 0.37 eV as compared to that for 3×3×2 cell result. The less stable configuration is then of S-type. These results are slightly different from those in [3], where the O configuration is the most stable. However the relative energy of BO configuration (E_{BO}-E_O) is only 0.04 eV. In the supercell containing 145 atoms the BS becomes more stable than O configuration and further increase of the cell size does not change the stability order of the configurations (see Table 4 and Fig. 2). The most stable is BO, the BS is

next with 0.10 eV higher formation energy, the O is 0.19 eV higher and, finally, the S configuration with 0.31eV higher formation energy. As can be seen from Fig. 2, the energy of O and S configurations are converged, while BO and BS are still slowly decreasing with the same slope. Further increase of the cell size will stabilize these configurations even more relative to O- and S- types. The sensitivity of energies to the supercell size in the directions along *c* and *b* basis vectors was examined for 6×5×5 supercell containing 301 atoms. According to the results obtained (see Table 4 and Fig. 2), the energy of BS SIA is very close to that for the 6×4×3 supercell. This is in accordance with the linear character of the BS defect. The formation energy of both BO and O defects decreases only slightly compared to the 6×4×3 supercell results in accordance with their planar and three-dimensional character. The largest drop in the formation energy is observed for the S defect, a linear defect oriented along the *c* direction. However, the increase of supercell size along *c* and *b* does not change the order of stability of SIA configurations, BO and BS being still the most stable.

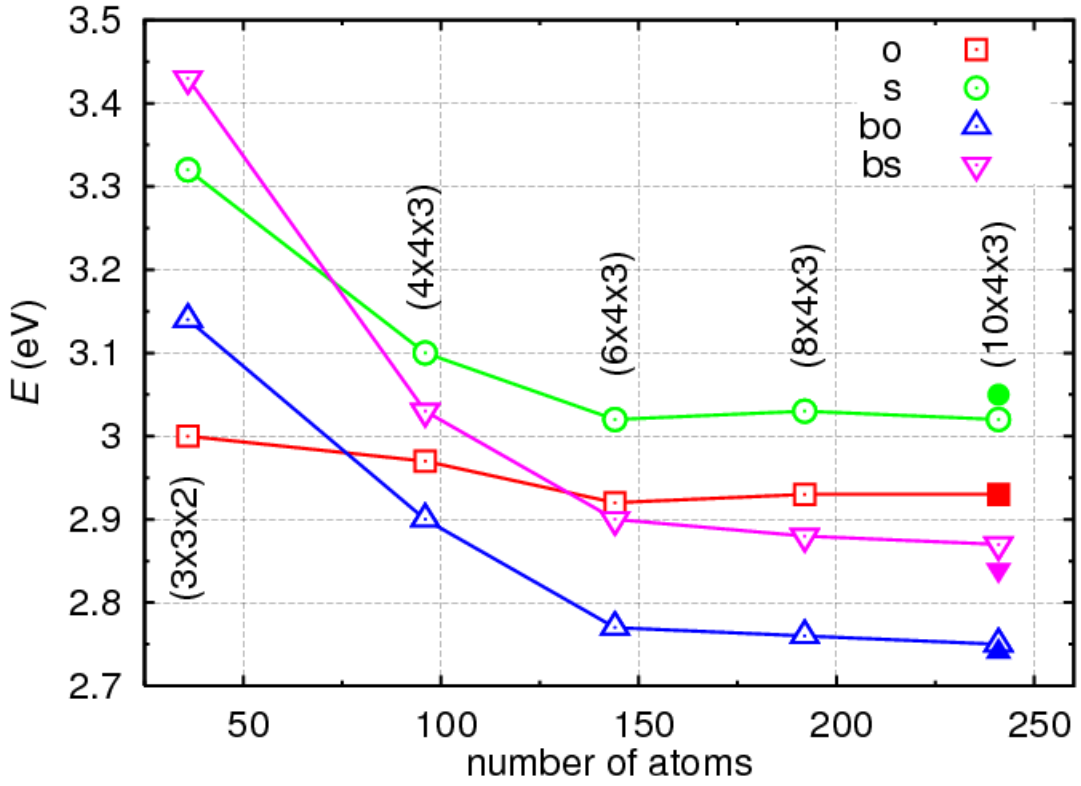

Figure 2. QE results for formation energy of different configurations of SIA defects in hcp Zr as a function of supercell size at equilibrium values of lattice parameter. The results shown by filled points correspond to the experimental lattice parameter.

In order to check sensitivity of the results obtained to the *c/a* ratio we repeated our calculation in the supercell with 241 atoms using the experimental value of the *c/a*=1.593 while keeping the same volume. The results obtained are presented in Table 4 and Fig. 2 (solid symbols). Similar to

the LDA value discussed above and in [2], the reduction of the *c/a* ratio increases the formation energy of S configuration, does not change the energy of O configuration and reduce the energy of basal configurations (BO and BS). Such modification reflects the fact that decreasing *c/a* ratio reduces the space available for relaxation in *c* direction, making the corresponding configurations less stable.

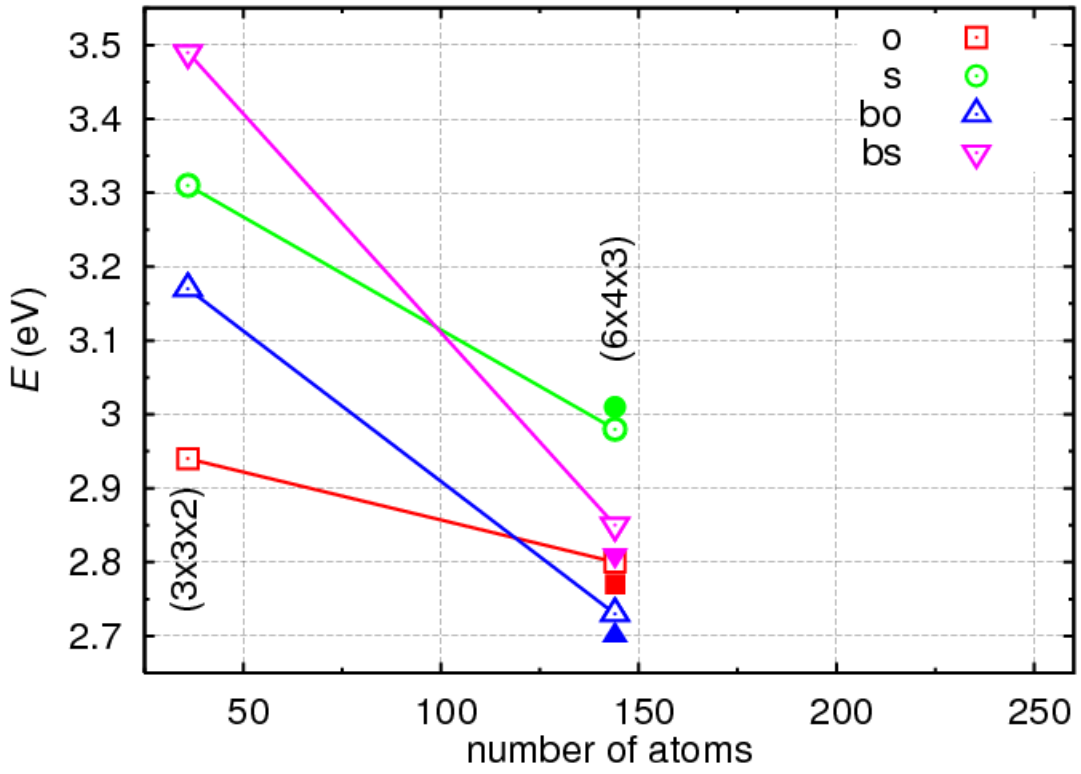

Figure 3. VASP results for formation energy of different configurations of SIA defects in hcp Zr as a function of supercell size at equilibrium values of lattice parameters. The results shown by filled points correspond to experimental lattice parameters.

The VASP results are presented in Table 2 and Fig. 3. Similar to the QE results, a further increase of the supercell size from 3×3×2 to 6×4×3 changes the order of stability, and the most stable SIA is now BO, while BS is still slightly higher in energy compared to O. However, the relative change of formation energy of BS- compared to O- type defects drops from 0.55 eV to 0.05 eV with increasing supercell size. It seems that, for the larger sizes, the most stable configurations are BO and BS in agreement with the QE calculations.

3. SUMMARY

The DFT methods were applied to study interstitial configurations in the hcp Zr. It was demonstrated that the relative stability of SIA configurations depends strongly on the simulation cell size, exchange-correlation functional and *c/a* ratio. The following conclusions were drawn based on the results obtained:

- Simulation cell size in the *a*-direction must be at least 8*a* to describe properly the relative stability of SIA configurations. Sensitivity to other directions is significantly weaker.
- The GGA approximation of the exchange-correlation functional describes *c/a* better than the LDA.
- Extrapolation of the results obtained to a large supercell and correct *c/a* predicts higher stability of basal configurations such as BO and BS over the out-of-plane configurations, such as O and S.
- The results have important consequences in possible diffusion modes for self-interstitial transport, making basal plane mechanisms most favorable. This is qualitatively consistent with experimental observations.

Further studies are needed to clarify diffusion modes for single SIAs and clusters. This work is in progress now together with collaboration with Edinburgh University (G. Ackland) and Ames Laboratories (M. Mendelev) in developing new interatomic potential for Zr, which will reproduce the features of interstitial type defects. Development of a new potential is crucial for understanding radiation effects in Zr and hcp metals. New empirical potential for Zr will be used in large scale atomistic simulation of defect diffusion, interaction of what with dislocation and grain boundaries, i.e. mechanisms that define microstructure evolution under irradiation.

REFERENCES

[1] S.I. Golubov, B.N. Singh, H. Trinkaus, J. Nucl. Mater. **276** 78 (2000).

[2] F. Willaime, J. Nucl. Mater. **323** 205 (2003).

[3] C. Domain, A. Legris, Phil. Mag. **85** 569 (2005).

[4] Y. Carlan, C. de, Regnard, M. Griffiths, D. Gilbon, C. Lemaignan, ASTM STP **1295** 638 (1996).

[5] A.J.E. Foreman, Report No. AERE-R-7135, UKAE Authority, Harwell, 1972.

[6] A.V. Barashev, S.I. Golubov, Phil. Mag. **90** 1787 (2010).

[7] Yu.N. Osetsky, A. Serra, B.N. Singh and S.I. Golubov, Philos. Mag. A **80** 2131 (2000).

[8] Yu.N. Osetsky, D.J. Bacon, A. Serra, B.N. Singh and S.I. Golubov, J. Nucl. Mater. **276** 65 (2000).

[9] Yu.N. Osetsky, A. Serra, B.N. Singh and S.I. Golubov, Philos. Mag. A **83**, 61 (2003).

[10] M.I. Mendelev, G.J. Ackland, Phil. Mag. Lett. **87** 349 (2007).

[11] P. Giannozzi, S. Baroni, *et. al*., J. Phys. Condens. Matter. **21** 395502 (2009).

[12] G. Kresse and J. Hafner, Phys. Rev. B **47** 558 (1993), *ibid*. **49** 14251 (1994).

[13] D. Vanderbilt, Phys. Rev. B **41** 7892 (1990).

[14] J. P. Perdew, K. Burke, M. Ernzerhof, Phys. Rev. Lett. **77** 3865 (1996).

[15] J. P. Perdew, Y. Wang, Phys. Rev. B **45** 13244 (1991).

[16] J. P. Perdew, A. Zunger Phys. Rev. B **23** 5048 (1991).

INTERNAL DISTRIBUTION

1. V. Barashev, barashevav@ornl.gov
2. S. I. Golubov, golubovsi@ornl.gov
3. G.I. Ice, icege@ornl.gov
4. D.B Kothe, kothe@ornl.gov
5. J. R. Morris, morrisj@ornl.gov
6. D. N. Nicholson, nicholsondm@ornl.gov
7. Yu. N. Osetsky, osetskiyyn@ornl.gov
8. M. Stocks, stocksgm@ornl.gov
9. R. E. Stoller, stollerre@ornl.gov
10. . B. Wirth, wirthbd@ornl.gov
11. S. J. Zinkle, zinklesj@ornl.gov
12. ORNL office of Technical Information

EXTERNAL DISTRIBUTION

1. C.A. English, Nexia Solutions, UK, colin.a.english@nnl.co.uk
2. D.J. Bacon, The University of Liverpool, Department of Engineering, Brownlow Hill, Liverpool, L69 3GH, UK, djbacon@liverpool.ac.uk
3. A. Serra, Universitat Politècnica de Catalunya, Dept. Matemàtica Aplicada III, ETSECCPB and CRNE, 08034, Barcelona, Spain, a.serra@upc.edu
4. Malcolm Griffiths, Atomic Energy of Canada Limited, Chalk Rover Laboratories, Chalk River, Ontario, Canada, griffithsm@aecl.ca
5. R.A. Holt, Department of Mechanical and Materials Engineering, Queen's University at Kingston, Ont., Canada K7L 1W9, holt@me.queensu.ca
6. Simon R. Phillpot, Department of Materials Science and Engineering, University of Florida, 100 Rhines Hall, PO Box 116400, Gainesville FL, 32611-6400, sphil@mse.ufl.edu
7. Donald R. Olander, Department of Nuclear Engineering, UC Berkeley, 4105 Etcheverry Hall MC 1730, Berkeley, CA 94720-1730, fuelpr@nuc.berkeley.edu
8. Arthur T. Motta, The Pennsylvania State University, 227 Reber Building, University Park, PA 16802, atm2@psu.edu
9. Donald Brenner, Department of Material Science and Engineering, North Carolina State University, Raleigh, NC, 276957907, brenner@ncsu.edu
10. Carlos N. Tome, MST-8, MS G755, Los Alamos National Laboratory, Los Alamos, New Mexico 87545, USA, tome@lanl.gov
11. B.P. Uberuaga, Materials Science and Technology Division, Los Alamos National Laboratory, Los Alamos, New Mexico 87545, USA, blas@lanl.gov
12. C. Domain, EDF-R&D Department MMC, Les Renardieres, F-77818 Moret sur Loint Cedex, France, christophe.domain@edf.fr

13. F. Willaime, Service de Recherches de Metallurgie Physique, DMN-SRMP, CEA Saclay, 91191 Gif-sur-Yvette, France, francois.willaime@cea.fr
14. Ishino Shiori, Editor of Journal of Nuclear Materials, ishino@k9.dion.ne.jp
15. H. Kaburaki, Nuclear Science and Engineering Directorate: Japan Atomic Energy Agency, Japan, kaburaki.hideo@jaea.go.jp
16. S.L. Dudarev, EURATOM/UKAEA Fusion Association, Culham Science Centre, Oxfordshire OX14 3DB, UK, Sergei.Dudarev@UKAEA.org.uk
17. A. Legris, Bâtiment C6 – 225, Unité Matériaux et Transformations, Bât. C6, Université Lille1, 59655 Villeneuve d'Ascq, France, alexandre.legris@univ-lille1.fr,
18. D. Nguyen-Manh, Materials Modeling Laboratory, Department of Materials, University of Oxford, Parks Road, Oxford OX1 3PH, manh.nguyen@materials.ox.ac.uk
19. M.W. Finnis, Imperial College London, Department of Materials, 105 Royal School of Mines, South Kensington Campus, m.finnis@imperial.ac.uk
20. A. Sutton, Imperial College London, Department of Materials, 105 Royal School of Mines, South Kensington Campus, a.sutton@imperial.ac.uk
21. F. Soisson, Service de Recherches de Metallurgie Physique, DMN-SRMP, CEA Saclay, 91191 Gif-sur-Yvette, France, Frederic.soisson@cea.fr
22. Sidney Yip, Department of Nuclear Science and Engineering, Massachusetts Institute of Technology, 77 Massachusetts Avenue, 24-107, Cambridge, MA 02139, syip@MIT.EDU
23. C.R Stanek, Los Alamos National Laboratory, Los Alamos, New Mexico 87545, USA, stanek@lanl.gov
24. G.S. Was, University of Michigan, Nuclear Engineering and Radiological Sciences, Cooley Building, Ann Ardor, MI 48109-2104, USA, gsw@umich. Edu
25. M.I. Mendelev, Materials and Engineering Physics, Ames Laboratory, US DOE, 207
26. Metals Development, Ames, IA, USA, mendelev@ameslab.gov
27. G.J. Ackland, 2502 JCMB, ICMCS School of Physics, University of Edinburgh, Edinburgh EH9 3JZ, G.J.Ackland@ed.ac.uk
28. D. Terentyev, Nuclear Materials Science, SCK-CEN, Boeretang 200, B-2400 Mol, Belgium, dterenty@sckcen.be
29. P. Vladimirov, Karlsruhe Institute of Technology (KIT), Institute for Applied Materials - Applied Materials Physics, Hermann-von-Helmholtz-Platz 1 IAM-AWP/MW, 76344
30. Eggenstein-Leopoldshafen, Germany, Pavel.Vladimirov@kit.edu
31. Stephen M. Foiles, Computational Materials Science and Engineering Dept., Sandia National Laboratories, Albuquerque, NM 87185-1411, foiles@sandia.gov
32. Arthur F. Voter, Theoretical Division, Los Alamos National Laboratory, Los Alamos, New Mexico 87545, USA, afv@lanl.gov